Time-Series Ensemble Photometry and the Search for Variable Stars in the Open Cluster M11

Jonathan R. Hargis[1]

San Diego State University, Department of Astronomy, 5500 Campanile Drive, San Diego, CA 92182

jhargis@eastern.edu

Eric L. Sandquist

San Diego State University, Department of Astronomy, 5500 Campanile Drive, San Diego, CA 92182

erics@sciences.sdsu.edu

David H. Bradstreet

Eastern University, Department of Physical Sciences, 1300 Eagle Road, St. Davids, PA 19087-3696

dbradstr@eastern.edu

ABSTRACT

This work presents the first large-scale photometric variability survey of the intermediate age ($\sim$ 200 Myr) open cluster M11. Thirteen nights of data over two observing seasons were analyzed (using crowded field and ensemble photometry techniques) to obtain high relative precision photometry. In this study we focus on the detection of candidate member variable stars for follow-up studies. A total of 39 variable stars were detected and can be categorized as follows: 1 irregular (probably pulsating) variable, 6 δ Scuti variables, 14 detached eclipsing binary systems, 17 W UMa variables, and 1 unidentified/candidate variable. While previous proper motion studies allow for cluster membership determination for the brightest stars, we find that membership determination is significantly hampered below $V = 15, R = 15.5$ by the large population of field stars overlapping

[1]Present address: Eastern University, Department of Physical Sciences, 1300 Eagle Road, St. Davids, PA 19087-3696

the cluster MS. Of the brightest detected variables that have a high likelihood of cluster membership, we find five systems where further work could help constrain theoretical stellar models, including one potential W UMa member of this young cluster.

Subject headings: binaries: eclipsing — delta Scuti — open clusters and associations: individual (M11)

1. Introduction

Our Galaxy's collection of open clusters presents an important population of stars for many areas of modern astrophysics, in particular for studies of variable stars and extrasolar planets. Because of the characteristics common to stars in open clusters (namely the age and chemical composition), much more information can be obtained for a particularly interesting cluster member star than could be otherwise deduced for an isolated field star. The high spatial density of stars in clusters allows for the opportunity to survey many stars at one time, a property important to increasing the probability of detection for extrasolar planetary transits. Other advantages of open cluster surveys for extrasolar planets have been summarized by von Braun et al. (2004). Observations of the various types of variable stars in clusters can provide the other critical remaining parameters necessary for studying the physics of stars: masses, radii, and luminosities. In the case of eclipsing binary systems and extrasolar planets, photometric observations of the eclipses yield constraints on the the orbital inclination and relative radii, the necessary compliments to radial velocity measurements that allow for the determination of the absolute system parameters. With the absolute properties measured, strong tests of structure and evolution become possible for both extrasolar planets (Baraffe et al. 2003; Chabrier et al. 2004; Burrows et al. 2004) and stars (for example Ribas 2003, Lacy et al. 2004).

In this paper we focus on the search for variable stars in the open cluster M11, identifying systems important for follow-up studies. In §2 we introduce the target and previous studies of this object. In §3 we describe the observations of the cluster. §4 details the data analysis, photometry, and search for variable stars. In §5 we describe the cluster color-magnitude diagram (CMD). The light curves for the detected variable stars are presented in §6. We give the conclusions and future work in §7.

2. The Target Cluster: M11

The open cluster M11 (NGC 6705, C 1848-063) is a rich and dense open cluster, containing on the order of several thousand stars. It is both relatively young and metal rich (see below), both of which are advantageous for searches for planetary transits; younger planets will be larger on average (causing a deeper transit, being more easily detectable) and have been observed to show a preference for metal-rich host stars (Santos et al. 2003). Here we present an overview of some relevant previous studies of M11 and the known variable stars in M11.

2.1. Previous Studies of M11

M11 has historically been the focus of cluster dynamics studies, but little work has been done on the variable star content. The earliest significant photometric study of M11 was conducted by Johnson, Sandage, & Wahlquist (1956), who derived a CMD from the UBV photographic data for stars brighter than V=15. They were the first to note the detection of a population of approximately 30 red giant stars, and found the cluster age to be intermediate between Praesepe and the Pleiades. Recent estimates of the age of M11 by Sung et al. (1999) find an age of $(200 - 250) \times 10^6$ yr. A study of the cluster dynamics for stars brighter than $V \sim 15$ magnitude was done by McNamara & Sanders (1977) based on the proper motion study by McNamara, Pratt, & Sanders (1977). These studies also noted the presence of a halo of low-mass stars, which was later confirmed by Solomon & McNamara (1980). Mathieu (1984) performed further photometry of M11 to form a complete and consistent sample of photometric measurements to compliment the proper motion measurements of McNamara, Pratt, & Sanders (1977). This study also examined, in detail, the cluster structure and dynamics of M11. It was not until the study by Brocato, Castellani, & Digiorgio (1993) that the cluster CMD was observed below $V \sim 15$; observations reached a limiting magnitude of $V \sim 22$. The most recent photometry has been presented by Sung et al. (1999), who covered an area of approximately $40\farcm0 \times 40\farcm0$ around the center of M11. They derive an unreddend distance modulus of $(V_o - M_v) = 11.55 \pm 0.10$ (distance = 2 kpc) and cluster radius of 16 arcminutes (= 9.5 pc for a distance of 2 kpc). Spectroscopic measurements have also been made of the red giant branch population of M11. Gonzalez & Wallerstein (2000) presented an abundance analysis of 10 red giant stars in M11, and deriving a metallicity of [Fe/H]=$+0.10 \pm 0.14$ from high-resolution spectra.

In the galaxy, the cluster is located (l =$27\fdg3$,$b = -2\fdg8$) near the Scutum star cloud and the Sagittarius-Carina arm, resulting in a very large contamination of the cluster CMD from the field population (Sung et al. 1999). As first noted by Mathieu (1984), the CMD

of the M11 field appears to have not only the typical red field star population, which is easily distinguished from the cluster main-sequence (MS), but also has a population of stars overlapping the cluster MS starting at approximately $V = 15$ and fainter. This has also been noted by Brocato, Castellani, & Digiorgio (1993), but is most clearly seen in Fig. 10 of Sung et al. (1999). Here, the population of stars is shown divided into 4 different sections: (1) the MS of M11, (2) the "blue" field star population, (3) field (lower division) and cluster (small upper division) giant stars, and (4) the "red" field star population. It is the population of field stars from group #2 that hampers membership estimation for many of the detected variables in this study. Without direct distance measurements, it is difficult to say with certainty that a given star falling in the overlap region (sections #1 and #2) is either a cluster member or member of the bluer field star population. As further confirmation that the stars in section #2 are not cluster members, Sung et al. (1999, Figure 5) derive a CMD for a region nearby M11, which clearly shows the bimodal field star population.

2.2. Known Variable Stars in M11

Observations of photometrically variable stars in this cluster and its vicinity have been rare. To date, no comprehensive study of the variable star population has been published. The most well-studied potential cluster member is BS Scuti, an Algol-type eclipsing binary ($P = 3.8$ d; Hall & Mallama 1974). The star IT Scuti, located much closer to the cluster center, is characterized as a slow irregular variable, although no light curve has been published. The only previously known, confirmed δ Scuti variable is V369 Scuti (McNamara, Pratt, & Sanders 1977 ID #624; $P = 0.223$ d; Hall & Mallama 1970). A recent survey for variability in M11 was performed by Paunzen et al. (2004), but the search concentrated on the brightest stars only. They note the detection of one variable star (ID #770 from McNamara, Pratt, & Sanders 1977) but do not indicate the type of variability detected nor present a light curve. Lastly, two spectroscopic binaries (IDs #926 and #1223, discovered in a radial velocity survey by Mathieu, Latham, Griffin, & Gunn 1986) were analyzed by Lee, Mathieu, & Latham (1989). We discuss our observations of these previously known and any suspected variable stars in §4.3.

3. Observations

The data for this study were obtained at the 1 m telescope at the Mount Laguna Observatory using a 2048×2048 CCD. In total, M11 was observed over the two observing seasons of 2002 and 2003 and 13 nights of data employed in this study are presented here.

Only observations where the nightly transparency (weather conditions) were good/excellent or photometric were used in this study. Table 1 presents the log of the observations; observing conditions are also noted, with error estimates to give some indication as to the photometric stability of the nightly data. Given a CCD plate scale of $0\farcs4$ pixel^{-1}, the total surveyed area around the cluster center was $13\farcm7 \times 13\farcm7$. In radial extent we have observed out to a radius of $6\farcm8$ from the cluster center; our observations have primarily covered the central portion of the cluster. Time-series observations (exposure times of 500 s were used in all monitoring data) were done exclusively in the R band to maximize the number of surveyed stars. Owing to the large readout time of the CCD, there was a delay of approximately 6.7 minutes between exposures. Observations were made on 02-03 September 2002 in the V band (exposure times of 10 s, 60 s and 300 s) for use in the construction of the $(V-R)$ color index.

4. Data Analysis

4.1. Data Reduction

Observations of the target cluster were reduced in the standard fashion, employing the IRAF[1] routines to correct the raw data. The bias level was subtracted using a fit to the overscan region of the CCD frames, and the overall noise level was further adjusted using a set of master bias frames. Pixel-to-pixel sensitivity variations were corrected through the use of flat fielding. Twilight flats were used where possible, and otherwise dome flats were employed.

4.2. Photometry

Photometry was performed using the DAOPHOT II/ALLSTAR suite of programs (Stetson 1987). Typically 80-100 bright, well-isolated stars were selected in construction of the frame point-spread function (PSF). The selection was also constrained by the division of the frame into 25 spatial bins, ensuring that the PSF stars were adequately spread across the frame (aiding in mapping any possible PSF variations across the image). In order to perform consistent photometry from night-to-night, one master star list of 11,267 stars (constructed from the best frames of 08/09 August 2002) was used uniformly throughout this study and only these stars were studied for variability. The large numbers of stars on each frame ensured excellent frame-to-frame positional transformations, with typical transformations

[1]Image Reduction and Analysis Facility is distributed by the National Optical Astronomy Observatories.

being accurate to better than 0.1 pixels. Night-to-night differences in the frame center and seeing conditions hinders measurements of every master star in every frame, but typically 9,000-10,500 stars were measured in each night of data.

In order to improve the relative photometry for the light curves, ensemble techniques (Sandquist, Latham, Shetrone, & Milone 2003, based on a general method by Honeycutt 1992) were used to determine a simultaneous, robust solution for the median magnitudes of all stars and the relative frame zero points. The initial solution resulted from the star-to-star comparisons determined from the positional transformations, and the solution was improved via iteration until neither the frame zeropoints nor the median magnitudes varied by more than 0.0003 magnitudes. Also included in the iterative procedure was the possibility that the magnitude residuals could be a function of frame x and y position. Second-order polynomials were fit to the magnitude residuals and the solution was subtracted during the iterations. At most, these corrections were only a few hundredths of a magnitude. Figure 1 displays the results of the ensemble techniques, showing the error in the median R magnitude as a function of median R magnitude.

4.3. Variable Star Detection

The search for variable stars in the data set was conducted using several techniques. Because transits of extrasolar planets exhibit characteristics different than typical eclipsing binary systems and pulsating variables (primarily in amplitude and variability signature), we optimize our detection methods to search for detached eclipsing binary systems, W UMa variables and δ Scuti and pulsating variables (that is, the higher-amplitude variables). Algorithms optimized for planetary transit searches and low-amplitude variables will be implemented in a subsequent study. As a general test of variability, the RMS variation about the R band median magnitude was calculated for each star. The results of this calculation are shown as a function of median R magnitude in Figure 2. Because this index is sensitive to outlier or spurious measurements the variability statistics I_{WS} from Welch & Stetson (1993) and J from Stetson (1996) were also employed, the statistics very often used when searching light curves for variability (Hebb et al. 2004; Bruntt et al. 2003; Mochejska et al. 2002). These indices use the correlation between closely-spaced (in time) data pairs to determine variability. More specifically, the I_{WS} statistic is given as

$$I_{WS} = \frac{1}{\sqrt{n(n-1)}} \sum_{i=1}^{n} \left((\frac{m_1 - m_{med}}{\sigma_1})(\frac{m_2 - m_{med}}{\sigma_2}) \right)_i ,$$

where $m_{1,2}$ are the first and second magnitude measurements of the ith data pair, $\sigma_{1,2}$ are the propogated errors of the magnitude differences, m_{med} is the calculated median magnitude,

and n is the total number of data pairs. The results for the I_{WS} calculation are shown in Figure 3. Also, the Lomb-Scargle power spectrum (Scargle 1982) was calculated between 1 h and 1 d (period sampling of 0.001 d) for every light curve in the data set, and the peak power and corresponding period were recorded. The Lomb-Scargle routine can be used in this way as a variability detection method. Being a Fourier analysis method, it is particularly sensitive to stars with periodically varying light curves resembling sine or cosine functions (such as the W UMa variables).

While the I_{WS} and J variability statistics are generally more sensitive to variability than the RMS search, the relatively high level of the noise in Figure 3 makes the detection of variables difficult. This arises, most likely, as a consequence of correlated seeing variations in a spatially crowded field when stars of comparable magnitude have a significant amount of overlap (see Sandquist & Shetrone 2003 and Hebb et al. 2004 for further discussion). To overcome this difficulty we calculate the I_{WS} and J statistics for each star *for each night* of data and examine those stars that have a large percentage change in the statistic from night-to-night. This will be particularly useful for detecting detached eclipsing binary systems, as the system will have little or no intrinsic variability on some nights (low I_{WS} or J when the system is not eclipsing) but will have relatively high variability scores (high I_{WS} or J when the system is eclipsing) on others. The results of this calculation are displayed in Figure 4, showing that 13 of the 14 detected detached eclipsing binary systems stand out easily above the noise. While the I_{WS} and J statistics are imperfect due to the crowded-field conditions, the use of multiple detection techniques (designed to identify specific types of variability) significantly increases the probability of detection. In general, variables were detected by viewing the light curves of stars above a reasonably low threshold in these statistics ($I_{WS} > 15$, $J > 15$, percentage variation of $J > 200\%$).

Once a variable star was detected, the period was determined using two slightly different techniques. Both the Lomb-Scargle (Scargle 1982) periodogram and the variation of the Lafler-Kinman algorithm (Lafler & Kinman 1965) by Deeming (Bopp, Evans, & Laing 1970) were calculated for each variable star that showed multiple events in the data set. The Lomb-Scargle calculation consists of the fitting of sine and cosine terms of various frequencies corresponding to possible periodicities in the data. The Lafler-Kinman search examines the light curve, folded on a trial period, for the minimization of differences between data points that are adjacent in phase space. Agreement between the two methods was excellent.

In order to confirm any suspected variable stars that may be in the M11 field and cross-reference our detections with previous studies, a search of the General Catalog of Variable Stars (Kholopov et al. 1998) was undertaken. This search revealed three suspected variables in cluster field: NSV 11410 (suspected long-period, slow irregular pulsating variable), 11402

(suspected long-period, slow pulsating variable), and 24615 (unspecified variable type). The star NSV 24615 is located near, if not coincident with, the brightest star in the cluster (HD 174512), which was saturated in our study. Searches around the coordinates of NSV 11410 and NSV 11402 did find nearby stars but no variability was detected. Given that the suspected variables are proposed slow variables, it remains plausible that the stars actually are variable in nature but that variability would be undetected over a short span of observations (3-10 days). No long-term (year-to-year) variability was noted in the light curves. Of the 6 previously known variable stars (see §2.2), 3 were saturated (V369 Sct and the 2 spectroscopic binaries of Lee, Mathieu, & Latham (1989)) and 2 were located outside the field of study (BS Sct and IT Sct). Thus, photometry was obtained only for the star ID #770 from McNamara, Pratt, & Sanders 1977. However, no sign of variability was detected. The star does appear to be a cluster member (by position on the CMD) but does not lie in the theoretical instability strip. Given that V369 Scuti (and possibly #770 from McNamara, Pratt, & Sanders 1977) is the only known variable star in the field of M11 covered in this study, all the variable stars in this study are new discoveries.

5. Color-Magnitude Diagram

One tool for estimating cluster membership for the detected variable stars is the cluster color-magnitude diagram (CMD). Figures 5 and 6 show the CMD of the M11 field derived from the measurement of 8,259 stars in this study; this is the total sample of stars measured in both the R and V images. Also marked are the detected variable stars from Table 2 and the theoretical instability strip from Pamyatnykh (2000). The theoretical isochrones from the Yonsei-Yale (Y^2) stellar evolution models (Kim, Demarque, Yi, & Alexander 2002) are shown for comparison (color-$T_{\rm eff}$ transformations from Lejeune, Cuisinier, & Buser 1998). The metallicity was chosen as $Z = 0.02$ in order to make a direct comparison to the CMDs of Sung et al. (1999). Figure 6 shows the theoretical isochrone from the Padova group (Girardi, Bressan, Bertelli, & Chiosi 2000 with color-$T_{\rm eff}$ transformations described in Girardi et al. 2002), generated for an identical metallicity and age ($\log t_{age} = 8.3$ yr). Because the observed data are uncalibrated, the magnitudes and colors were shifted to match the theoretical isochrones. The derived unreddened distance modulus from Sung et al. (1999) was used to shift the Y^2 models to the apparent magnitude scale by adding the appropriate amount of reddening, assuming $E(B-V) = 0.428$ and $R = 3.1$ (Sung et al. 1999). This shifting of the observed data was done only for convienent plotting. We have not produced standard magnitudes, and we have not done anything requiring standard magnitudes.

As first noted by Mathieu (1984), the CMD of the M11 field appears to have not only the

typical red field star population, which is easily distinguished from the cluster main-sequence (MS), but also has a population of stars overlapping the cluster MS starting at approximately $V \sim 15$ ($R \sim 15.5$) and fainter. The field population is bimodal; there exists a "red" field star population ($(V-R)_o > 0.7$) and a "blue" field star population ($0.25 < (V-R)_o < 0.7$). The blue field star population hampers the identification of cluster members via the CMD for many of the detected variable stars in this study. Membership for individual variables will be discussed in §6.1 – 6.3.

6. Light Curves

6.1. δ Scuti Variables

In Figure 7, we show sample light curves for the 6 δ Scuti variables (IDs 320, 331, 536, 614, 619, and 6870) detected in this study. As can be seen in Figures 5 and 6, the cluster MS just begins intersects the faint edges of the theoretical instability strip (Pamyatnykh 2000) and so a δ Scuti population in this cluster is not surprising. Given the bright magnitude of these objects, membership probabilities are available from the McNamara, Pratt, & Sanders (1977) proper motion study; these are given in Table 2.

Particularly interesting is the variable ID 6870, which shows an amplitude of variation more than an order of magnitude greater than the five other detected δ Scuti variables. This star is likely a member of a sub-class of δ Scuti variables known as high amplitude δ Scuti variable stars (see Rodriguez 2004 and references therein). These differ from regular δ Scuti pulsators in that they have significantly larger amplitudes of variation (often greater than 0.3 magnitudes), appear to have only one or two radial pulsation modes (and no non-radial modes), and have slower rotation speeds (Rodríguez et al. 1996). ID 6870 is likely a field population main-sequence star, as δ Scuti variability would position the star inside or near the instability strip if it were a cluster member. Use of the period-density relation for δ Scuti stars (Breger 2000) yields a stellar density typical of MS stars.

6.2. Semi-detached and Detached Eclipsing Binaries

In Figure 8 we show the light curves for the 14 detached eclipsing binary systems detected in this study. Multiple eclipses were detected for 6 of the 13 systems, and hence periods were determined (listed in Table 2) for these systems. IDs 1814 and 4678 show characteristics of RS CVn-type eclipsing binaries, namely the large light curve scatter and rapidly changing light curve shapes (presumably due to quickly changing star spot activity). IDs 1583 and

3096 show light curves typical of Algol-type semi-detached systems while IDs 1340 and 1938 show little or no outside of eclipse light variations and are likely detached systems. In 8 of the 14 detected systems only one or two events were detected and therefore periods could not be determined.

In terms of cluster membership, we are only able to make reasonable judgments about the brightest stars owing to the overlap of the field star population noted in §5. Both IDs 729 and 977 show positions on the CMD consistent with cluster membership. The proper motion study by McNamara, Pratt, & Sanders (1977) further supports this conclusion where they determine membership probabilities of 81% and 52%, for IDs 729 and 977, respectively. While the McNamara, Pratt, & Sanders (1977) finds a very low membership probability for ID 1026 (7%), the position of this system near the cluster MS suggests it is likely a cluster member. The stars ID 1340, 1814, and 1938 show positions near the equal mass binary sequence, but given the presence of the overlapping field star population below $R =\sim 15.5$, we are unable to definitively claim cluster membership without further data on these or fainter systems. Finally, although ID 2119 shows total eclipses in its light curve, its position in the CMD indicates that it is almost certainly a part of the field population, so we have not pursued it further.

6.3. W Ursae Majoris Variables

In Figure 9 we show the light curves for the 17 W UMa variables (contact binary systems) detected in this study. The differences in shapes of the light curves of these systems are primarily due to three main effects: the orbital inclination (influencing the depth of eclipses), the degree of fillout of the Roche geometry (influencing the steepness of the eclipses and the "broadness" of the light curves at quadratures), and the mass ratio. In order to make a judgment regarding the geometric configuration of these systems, we modeled the data of the brightest systems using the *Binary Maker 3* light curve synthesis program (Bradstreet & Steelman 2002). Given the lack of spectroscopically determined mass ratios, elaborate fitting of the data using the Wilson-Devinney code (Wilson & Devinney 1971, hereafter WD) or other fitting routines is not worthwhile for those systems that do not exhibit total eclipses. A mass ratio of $q = 0.4$ was assumed when modeling those systems. Modeling shows that these variables can easily be described as contact binary systems. We discuss the light curves and synthetic models of IDs 3025 and 5274 below, both of which show evidence for total eclipses. In the case of totally-eclipsing light curves the assumption of an arbitrary mass ratio is unnecessary; the duration of totality strongly constrains the possible combinations of inclination and mass ratio.

The CMD presents the primary tool by which to estimate cluster membership for these contact systems. It is likely that the detected systems are members of the field population for two reasons: (1) the large spatial separation of systems from the cluster center and (2) positions on the CMD which are inconsistent with the cluster MS and binary sequence. In the first case, we find that the radial distances from cluster center (column 5, Table 3) are likely inconsistent with cluster membership in all but five (IDs 243, 2740, 3408, 8146, 8641) of the 17 cases. Figure 10 shows the positions of the detected W UMa systems relative to the brightest non-varying cluster stars ($R > 15$), the cluster center, and the cluster half-mass radius (as determined by Mathieu 1984). For reference, the adjacent panel shows the positions of the other detected variables. These indicate that the W UMa systems are more concentrated within the field population than the other 3 types of detected variables, especially considering that dynamical evolution should concentrate member binary systems to the cluster center. In the second case, only 3 of the 17 W UMa systems (IDs 5480, 8066, 8641) have CMD positions between the cluster MS and binary sequence. While this could be indicative of cluster membership, we stress that the possible presence of differential reddening, statistically uncertain V magnitudes that contribute to the $(V - R)$ position on the CMD, and the overlapping field star population in the CMD complicate these judgments. In summary, given the two criteria above for consideration of cluster membership, only ID 8641 appears to have both a radial distance from cluster center and CMD position consistent with membership. While ID 2740 is located spatially close to cluster center, it is not easily distinguishable from the field star population on the CMD. No V measurement was obtained for ID 3408 due to the crowded nature of the M11 field, and hence no CMD information is available for that system. Because proper motion data is available for ID 243, we discuss the possibility of cluster membership below.

ID 3025 Short total eclipses are evident in the light curve of the variable ID 3025 in Fig. 11. Initial models were generated using *Binary Maker 3* and the WD code was used to refine these input model parameters. Figure 11 shows the observed light curve of ID 3025 (data have been binned into 200 normal points), the 3-D model generated from *Binary Maker 3*, and the WD solution. The model parameters (adopted and fit) are given in Table 4. The ephemeris (probable errors in parentheses) derived from the period study is: time of primary minimum=2452495.74767+0.441864(3). Our analysis indicates that ID 3025 is likely a typical A-type contact system, the larger star being hotter by approximately 100 K.

ID 5274 Individual nights of data for the variable ID 5274 show evidence of a total primary eclipse. An initial model was generated using *Binary Maker 3*, biasing the solution to one with a combination of mass ratio, fillout and inclination that matched the total eclipse. To take a more unbiased approach to the analysis we used this initial model as input to WD to derive a final differential corrections solution. Figure 12 shows the observed light

curve of ID 5274 (data have been binned into 200 normal points), along with these two solutions. The model parameters are given in Table 5. We find the WD solution highly influenced by (1) the large scatter in the light curve and (2) the significant asymmetry in the quadratures (likely due to the presence of cool spots). The WD corrections appear to be favoring a lower inclination solution in order to fit the shoulders of quadrature around phase 0.25. Thus, the WD solution represents an averaging of the two different brightnesses at quadrature. We did not model the presence of spots in this system because of the large scatter and lack of multibandpass observations. Our analysis finds ID 5274 to be a W-type contact binary system, the larger star being cooler by approximately 450 K. The ephemeris (probable errors in parentheses) derived from the period study is: time of primary minimum=2452796.92403+0.3468800(1). While we believe the system to be totally eclipsing, the lower inclination solution calls into question the derived mass ratio. Given the large scatter in the data and the uncertainties in the inclination/mass ratio combination, these models should be considered preliminary. Higher precision, multifilter light curves are necessary to further constrain these models.

ID 243 For the variable ID 243, independent cluster membership information is available from the proper motion study of McNamara, Pratt, & Sanders (1977), who find a moderate probability of membership (62%). This object is also radially located within the cluster half-mass radius adding further circumstantial evidence that this variable could be a cluster member. In terms of location on the CMD, this object falls inside the theoretical instability strip. It is unlikely, however, that this object is a cluster pulsating δ Scuti variable since the necessary period ($P = 0.43289$ d for 1 pulse per cycle) would be at least an order of magnitude greater than typical δ Scuti variables. The light curve of ID 243 is consistent with those of very low inclination W UMa variables, and given the longer period of the system, this presents a more reasonable interpretation of the variability. Spectroscopic data would help in the resolution of the true nature of this system and refine the question of membership in M11.

Despite this circumstantial evidence for cluster membership, the young age of the cluster may preclude a population of W UMa members. The presence of contact binary stars in young clusters would likely require either (1) the formation of systems with small initial orbital separations, such that an angular momentum loss mechanism could bring the stars into contact on a short timescale (Guinan & Bradstreet 1988), or (2) the birth of binary systems in the contact phase. While these scenarios may not be unlikely, the detection of contact systems in young or intermediate age open clusters (ages less than ~ 1 Gyr) remains elusive. Observational difficulties result from the presence of faint W UMa variables in a bright, crowded field; image exposure times must be long to detect faint variables, but longer exposure times result in over-exposure of the brightest stars.

6.4. Candidate Variables

In this study, two variable stars were detected that could not be readily identified from the shape of the light curves. The data are shown in Figure 13 and we describe them individually below.

ID 220 This object, while located within the theoretical instability strip on the cluster CMD (see Figure 6), has a membership probability of 0% as determined by McNamara, Pratt, & Sanders (1977). However, the proper motion study by Su et al. (1998) finds a membership probability of 100%. Photometric variations are observed on both long (as shown in Figure 13) and short timescales (at nearly the Nyquist frequency of the observations, $\sim$ 10 min). The presence of the short or long term variability was observed to differ from night-to-night; thus, it is unclear to which category of variable stars this object belongs. The appearance of multiple frequencies of variability and possible cluster membership (and hence a CMD position in the instability strip) tends to argue for a type of pulsating variable.

ID 708 This object was near the edge of the reference frame and hence was only measured in two nights of observing. No V band data were obtained for this star (since it was located just outside the reference frame), so the position on the CMD was not determined. It is unclear if the minima in the light curves are a result of eclipses (from either a detached eclipsing binary or contact binary system) or minimums in stellar pulsation.

7. Conclusions

In conclusion, this work presents the first large-scale photometric variability survey of the intermediate age ($\sim$ 200 Myr) open cluster M11. A total of 39 variable stars were detected and can be categorized as follows: 1 irregular (probably pulsating) variable, 6 δ Scuti variables, 14 detached eclipsing binary systems, 17 W UMa variables, and 1 unidentified/candidate variable. While previous proper motion studies (McNamara, Pratt, & Sanders 1977; Su et al. 1998) allow for cluster membership determination for the brightest stars, we find that the membership determination is significantly hampered below $V = 15, R = 15.5$ by the large population of field stars at similar photometric colors to the cluster MS.

Of the detected systems, several are worth noting for follow-up work. First, three detached eclipsing binaries (IDs 729, 977, 1026) are likely cluster members, but will require further photometric data to deduce the orbital period. Given more photometric and spectroscopic data on these systems, the derivation of the absolute parameters (masses and radii) could be useful in constraining theoretical stellar models. Second, of the six δ Scuti variables detected in this study (all of which are likely cluster members), further studies of the pulsa-

tion periods of IDs 536 and 614 would make excellent tests of the blue edge of the theoretical instability strip. Third, the W UMa variable ID 243 is a potential cluster member. If it can be confirmed that it is a cluster member and also a W UMa variable, it would be the first confirmation of a contact system in an open cluster younger than 0.7 Gyr. Further photometric study can help confirm the orbital period and light curve variations, while spectroscopic observations will be critical to confirming the binary nature of the system. If the system is in fact a contact binary, it is likely that the spectrum will show double lines. Lastly, we find two W UMa variables that exhibit total eclipses in their light curves and present preliminary models using *Binary Maker 3* and Wilson-Devinney differential corrections. While the total secondary eclipse of the field W UMa variable ID 3025 constrains the mass ratio of the system photometrically, a spectroscopic mass ratio would be more appropriate and help in determination of the absolute parameters of the system. Inspection of the light curve of ID 5274 yields evidence of a total primary eclipse. However, the large scatter in the data and asymmetries in the light curve favor a lower inclination solution that forces a partial eclipse model. Futher high precision, multifilter light curves and a spectroscopic mass ratio are necessary to further refine our preliminary models of this system.

This research has made use of the SIMBAD database, operated at CDS, Strasbourg, France. This project has also made use of the CALEB database (http://caleb.eastern.edu/). J.R.H. wishes to thank Paul Etzel both for useful conversations regarding variable stars and the generous allocation of observing time at Mt. Laguna Observatory. J.R.H. also wishes to thank Slavek Rucinski for useful conversations about W UMa variables in young open clusters. The authors would like to thank the referee for the useful comments which have greatly improved this paper. This work has been partially funded through grant AST 00-98696 from the National Science Foundation to E.L.S. and Michael Bolte, and through a Research, Scholarship, and Creative Activity (RSCA) grant from San Diego State University to E.L.S.

REFERENCES

Baraffe, I., Chabrier, G., Barman, T. S., Allard, F., & Hauschildt, P. H. 2003, A&A, 402, 701

Bopp, B. W., Evans, D. S., & Laing, J. D. 1970, MNRAS, 147, 355

Bradstreet, D. H. & Steelman, D. P. 2002, Bulletin of the American Astronomical Society, 34, 1224

Breger, M. 2000, ASP Conf. Ser. 210: Delta Scuti and Related Stars, 210, 3

Brocato, E., Castellani, V., & Digiorgio, A. 1993, AJ, 105, 2192

Bruntt, H., Grundahl, F., Tingley, B., Frandsen, S., Stetson, P. B., & Thomsen, B. 2003, A&A, 410, 323

Burrows, A., Hubeny, I., Hubbard, W. B., Sudarsky, D., & Fortney, J. J. 2004, ApJ, 610, L53

Chabrier, G., Barman, T., Baraffe, I., Allard, F., & Hauschildt, P. H. 2004, ApJ, 603, L53

Girardi, L., Bertelli, G., Bressan, A., Chiosi, C., Groenewegen, M. A. T., Marigo, P., Salasnich, B., & Weiss, A. 2002, A&A, 391, 195

Girardi, L., Bressan, A., Bertelli, G., & Chiosi, C. 2000, A&AS, 141, 371

Gonzalez, G. & Wallerstein, G. 2000, PASP, 112, 1081

Guinan, E. F., & Bradstreet, D. H. 1988, NATO ASIC Proc. 241: Formation and Evolution of Low Mass Stars, 345

Hall, D. S. & Mallama, A. D. 1970, PASP, 82, 830

Hall, D. S. & Mallama, A. D. 1974, Acta Astronomica, 24, 359

Hebb, L., Wyse, R. F. G., & Gilmore, G. 2004, AJ, 128, 2881

Honeycutt, R. K. 1992, PASP, 104, 435

Johnson, H. L., Sandage, A. R., & Wahlquist, H. D. 1956, ApJ, 124, 81

Kholopov, P. N., et al. 1998, Combined General Catalogue of Variable Stars, 4.1 Ed (II/214A). (1998), 0

Kim, Y., Demarque, P., Yi, S. K., & Alexander, D. R. 2002, ApJS, 143, 499

Lacy, C. H. S., Claret, A., & Sabby, J. A. 2004, AJ, 128, 1840

Lafler, J. & Kinman, T. D. 1965, ApJS, 11, 216

Lee, C. W., Mathieu, R. D., & Latham, D. W. 1989, AJ, 97, 1710

Lejeune, T., Cuisinier, F., & Buser, R. 1998, A&AS, 130, 65

Mathieu, R. D. 1984, ApJ, 284, 643

Mathieu, R. D., Latham, D. W., Griffin, R. F., & Gunn, J. E. 1986, AJ, 92, 1100

McNamara, B. J., Pratt, N. M., & Sanders, W. L. 1977, A&AS, 27, 117

McNamara, B. J. & Sanders, W. L. 1977, A&A, 54, 569

Mochejska, B. J., Stanek, K. Z., Sasselov, D. D., & Szentgyorgyi, A. H. 2002, AJ, 123, 3460

Pamyatnykh, A. A. 2000, ASP Conf. Ser. 210: Delta Scuti and Related Stars, 215

Paunzen, E., Zwintz, K., Maitzen, H. M., Pintado, O. I., & Rode-Paunzen, M. 2004, A&A, 418, 99

Ribas, I. 2003, A&A, 398, 239

Rodríguez, E., Rolland, A., López de Coca, P., & Martín, S. 1996, A&A, 307, 539

Rodriguez, E. 2004, Communications in Asteroseismology, 145, 42

Sandquist, E. L., Latham, D. W., Shetrone, M. D., & Milone, A. A. E. 2003, AJ, 125, 810

Sandquist, E. L. & Shetrone, M. D 2003, AJ, 125, 2173

Scargle, J. D. 1982, ApJ, 263, 835

Santos, N. C., Israelian, G., Mayor, M., Rebolo, R., & Udry, S. 2003, A&A, 398, 363

Solomon, S. J. & McNamara, B. J. 1980, AJ, 85, 432

Stetson, P. B. 1987, PASP, 99, 191

Stetson, P. B. 1996, PASP, 108, 851

Su, C.-G., Zhao, J.-L., & Tian, K.-P. 1998, A&AS, 128, 255

Sung, H., Bessell, M. S., Lee, H., Kang, Y. H., & Lee, S. 1999, MNRAS, 310, 982

van Hamme, W. 1993, AJ, 106, 2096

von Braun, K., Lee, B. L., Seager, S., Yee, H. K. C., Mallen-Ornelas, G., & Gladders, M. D. 2004, AJ, submitted

Welch, D. L. & Stetson, P. B. 1993, AJ, 105, 1813

Wilson, R. E. & Devinney, E. J. 1971, ApJ, 166, 605

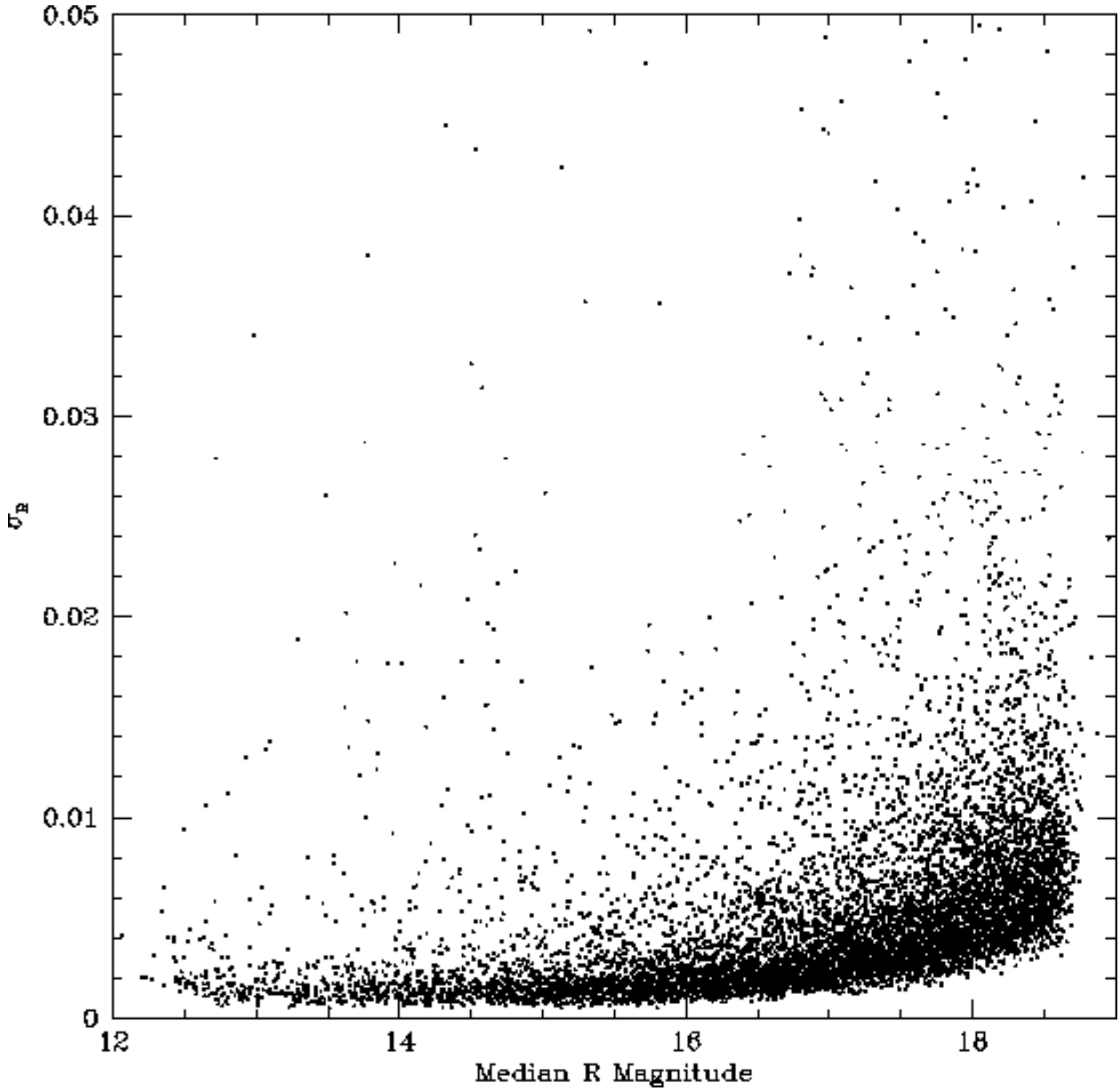

Fig. 1.— Results of the ensemble procedure used to interatively determine the nightly zero-points and median magnitudes. Shown is the error in the median R magnitude σ_R as a function of median R magnitude.

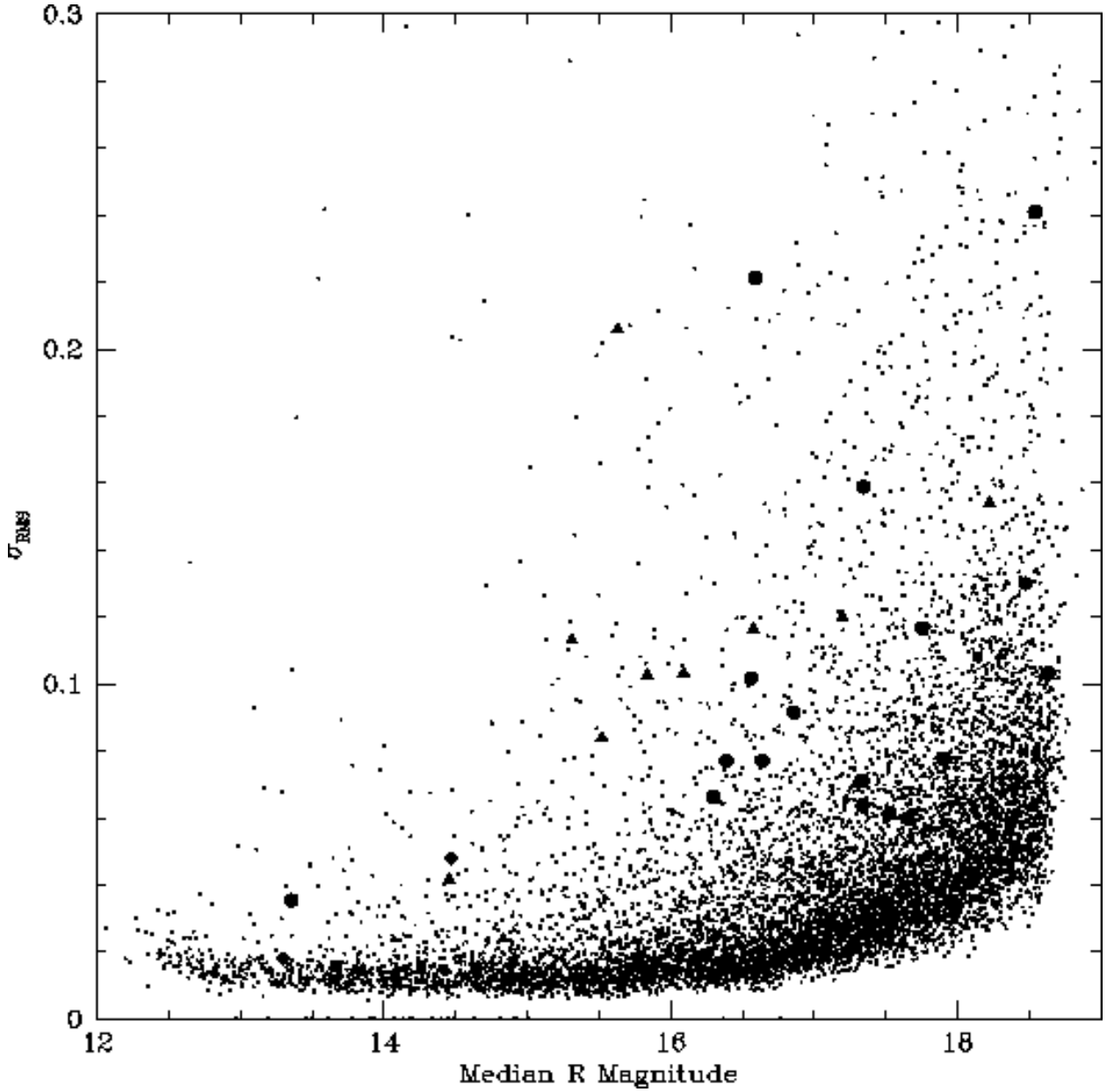

Fig. 2.— Results of the calculation of the RMS variation σ_{RMS} about the median R magnitude for the total data set.The detected variables are denoted as follows: *Filled Square*-δ Scuti or pulsating variable, *Filled Circle*-W UMa variable, *Filled Triangle*-detached eclipsing binary, and *Filled Diamond*-unknown/unidentified variable.

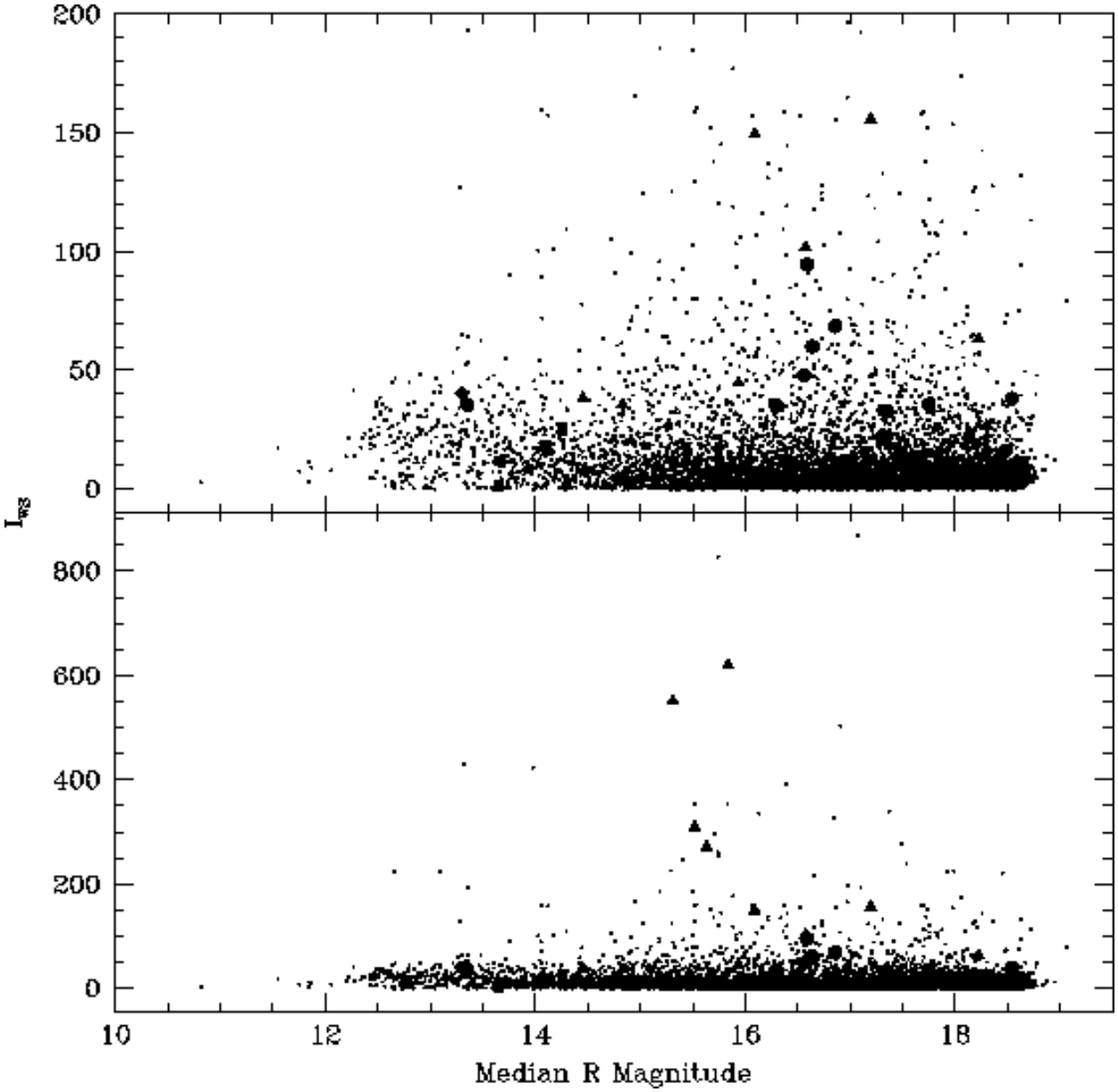

Fig. 3.— Results of the calculation of the Welch-Stetson variability index I_{WS} as a function of median R magnitude for the total data set. The top panel is identical to the bottom, highlighting the low scoring variables. The detected variables are denoted as follows: *Filled Square*-δ Scuti or pulsating variable, *Filled Circle*-W UMa variable, *Filled Triangle*-detached eclipsing binary, and *Filled Diamond*-unknown/unidentified variable.

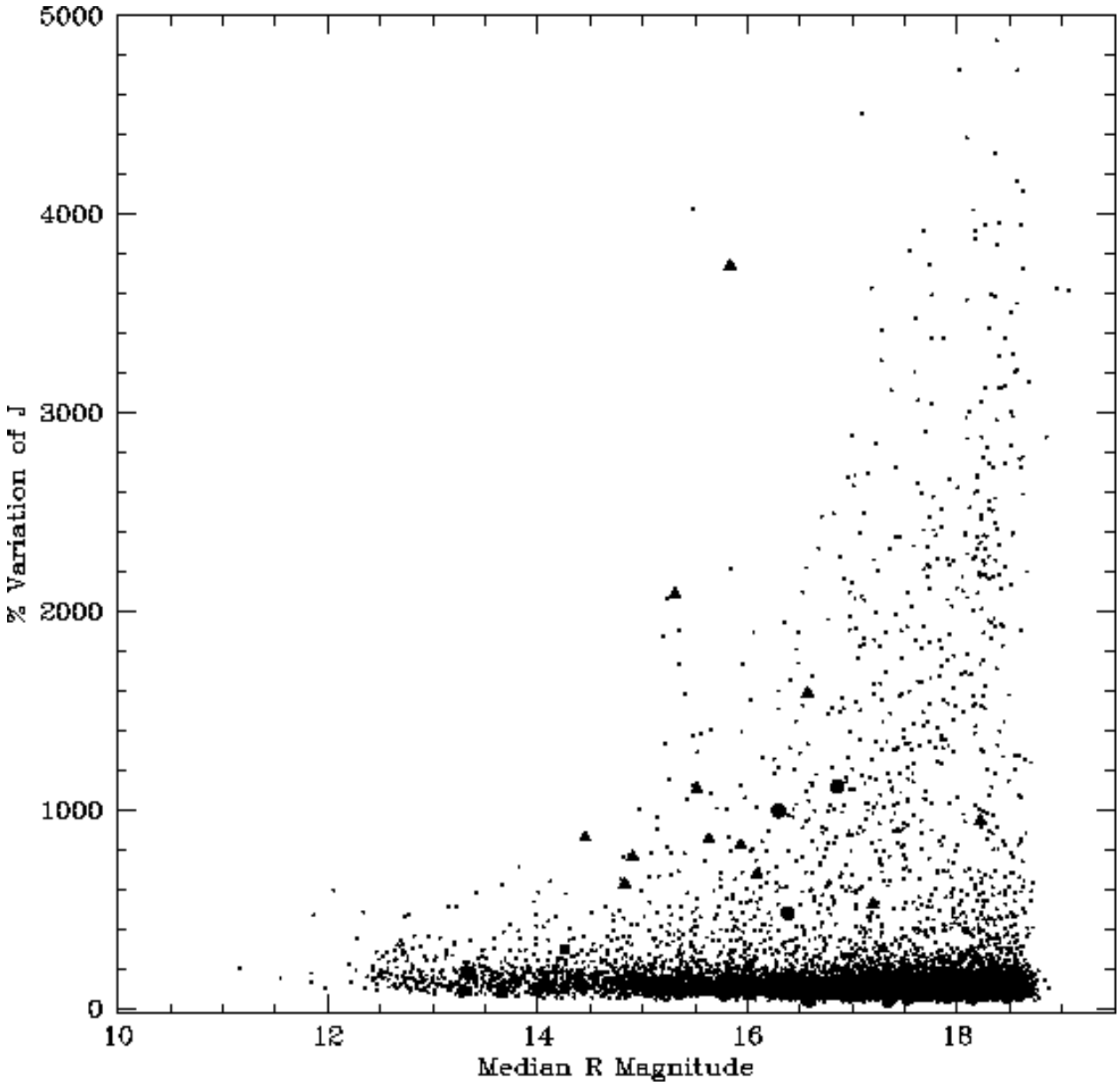

Fig. 4.— Results of the calculation of the percentage of night-to-night changes in the Stetson J variability statistic as a function of median R magnitude for the total data set. This calculation will be sensitive to the detection of eclipsing binary stars; see §4.3 for details. The detected variables are denoted as follows: *Filled Square*-δ Scuti or pulsating variable, *Filled Circle*-W UMa variable, *Filled Triangle*-detached eclipsing binary, and *Filled Diamond*-unknown/unidentified variable.

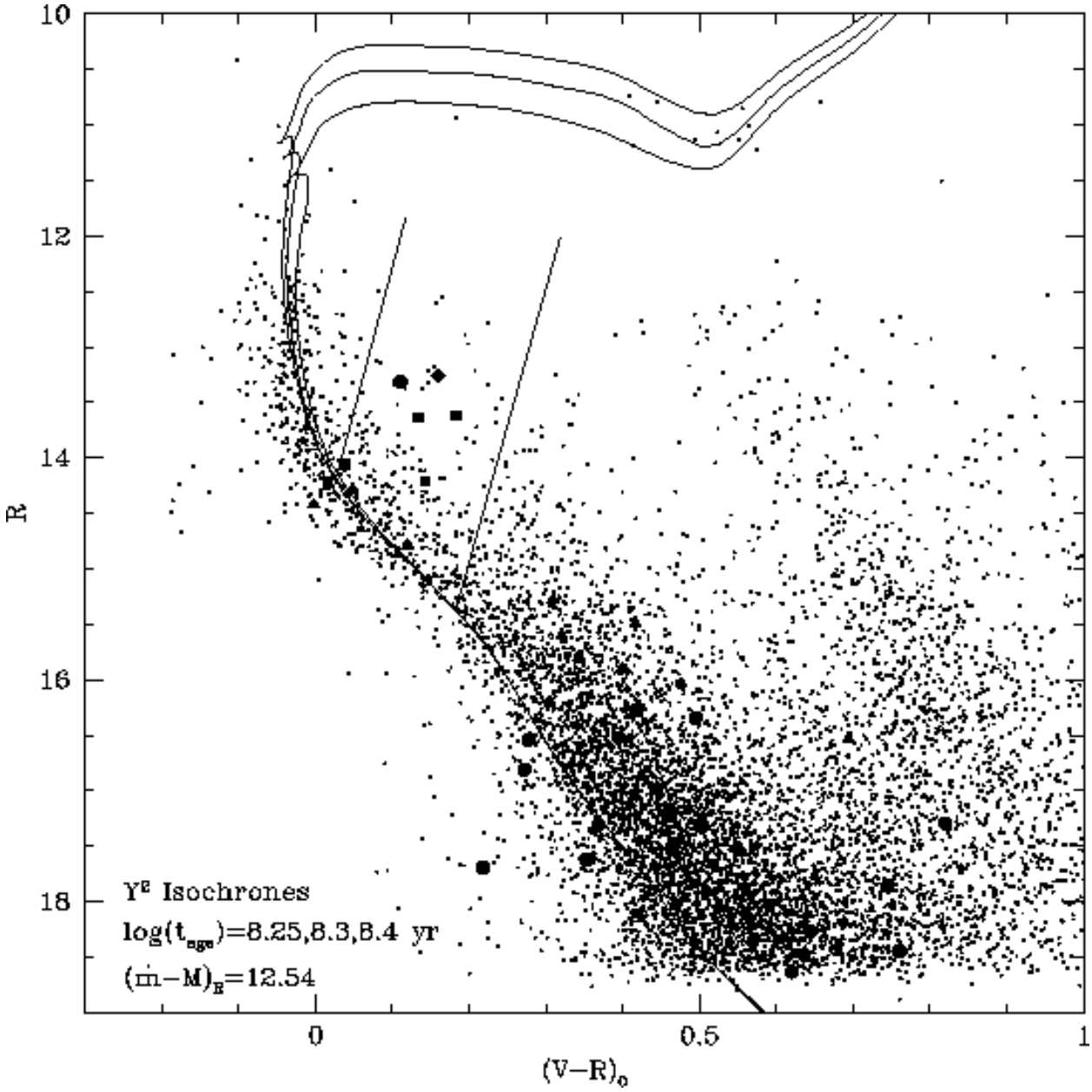

Fig. 5.— $R, (V - R)$ color-magnitude diagram. Overlaid are the Y^2 theoretical isochrones and the theoretical instability strip from Pamyatnykh (2000). The detected variable stars are denoted as follows: *Filled Square*-δ Scuti or pulsating variable, *Filled Circle*-W UMa variable, *Filled Triangle*-detached eclipsing binary, and *Filled Diamond*-unknown/unidentified variable.

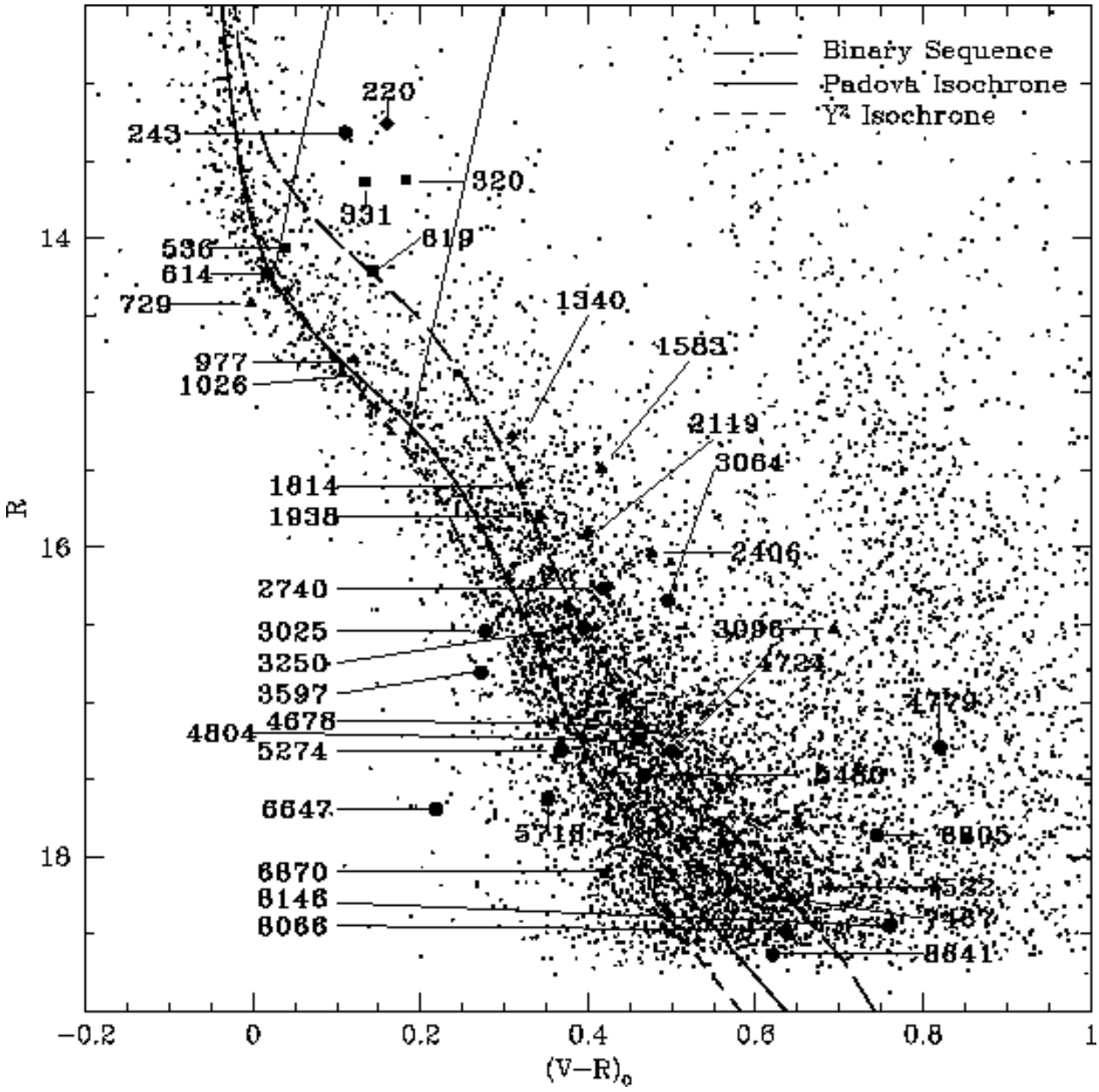

Fig. 6.— $R, (V - R)$ color-magnitude diagram with variable stars identified. Overlaid are the theoretical isochrone from the Padova and Y^2 groups, the theoretical binary sequence, and theoretical instability strip from Pamyatnykh (2000). The symbols are the same as in Fig. 5.

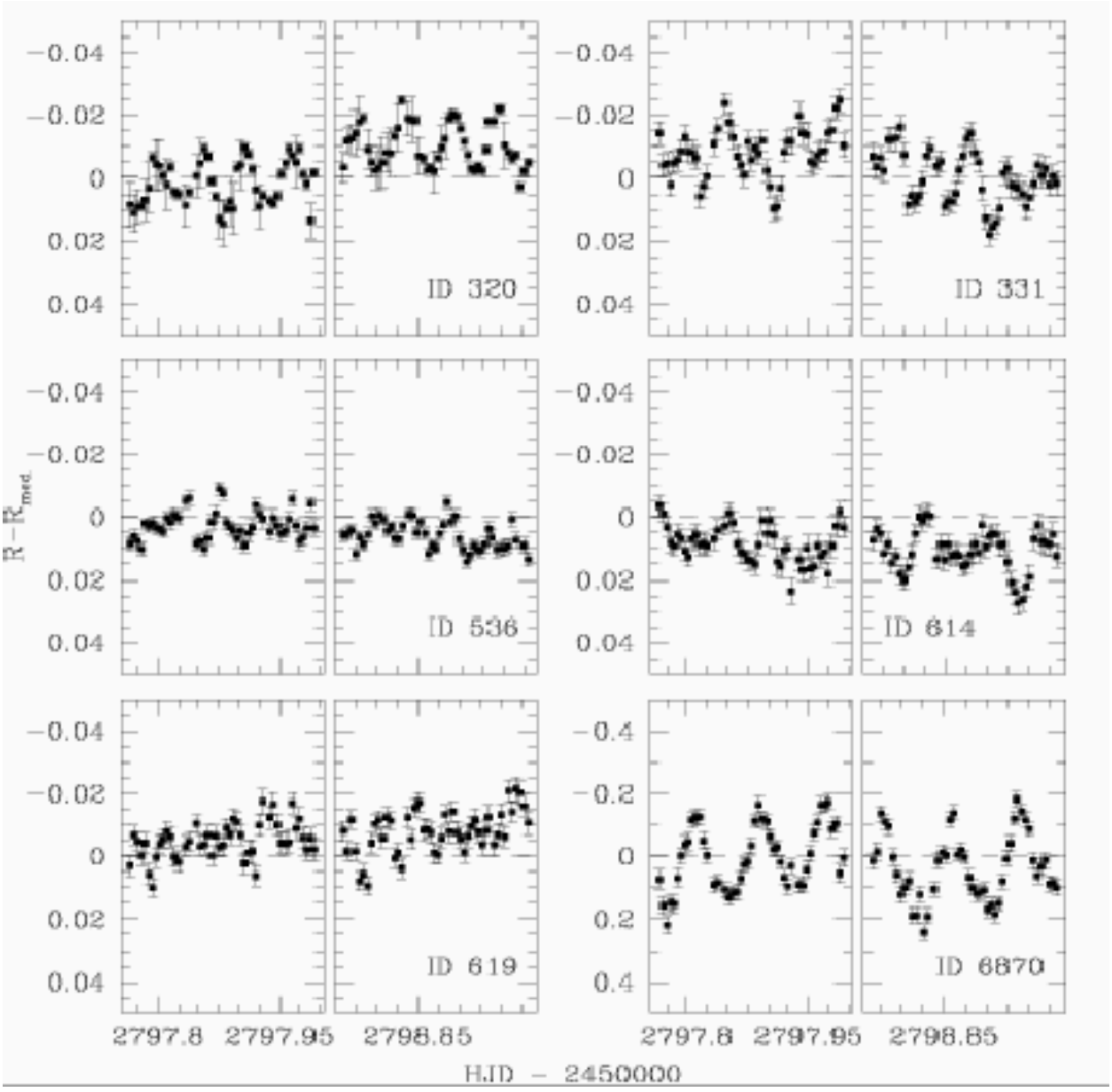

Fig. 7.— Light curves for the six δ Scuti variables detected in this study. Two nights of data are shown for each star.

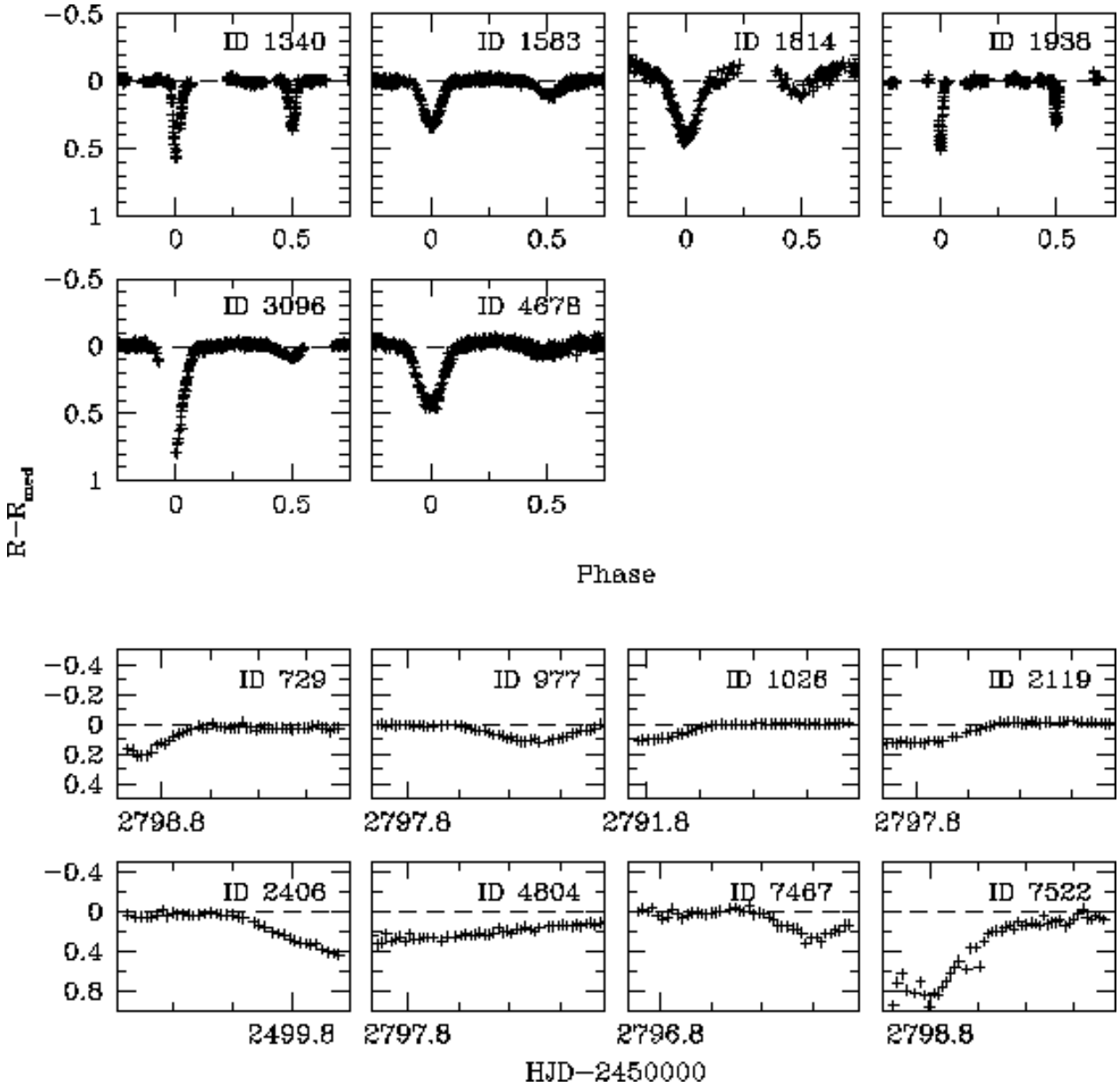

Fig. 8.— Light curves (types EA or EB) for eclipsing binary systems detected in this study. The top panels show those eclipsing binaries where multiple eclipses were observed, allowing for the determination of an ephemeris. The bottom panels shows eclipse events for those systems where only one or two eclipses were detected and no ephemeris could be determined.

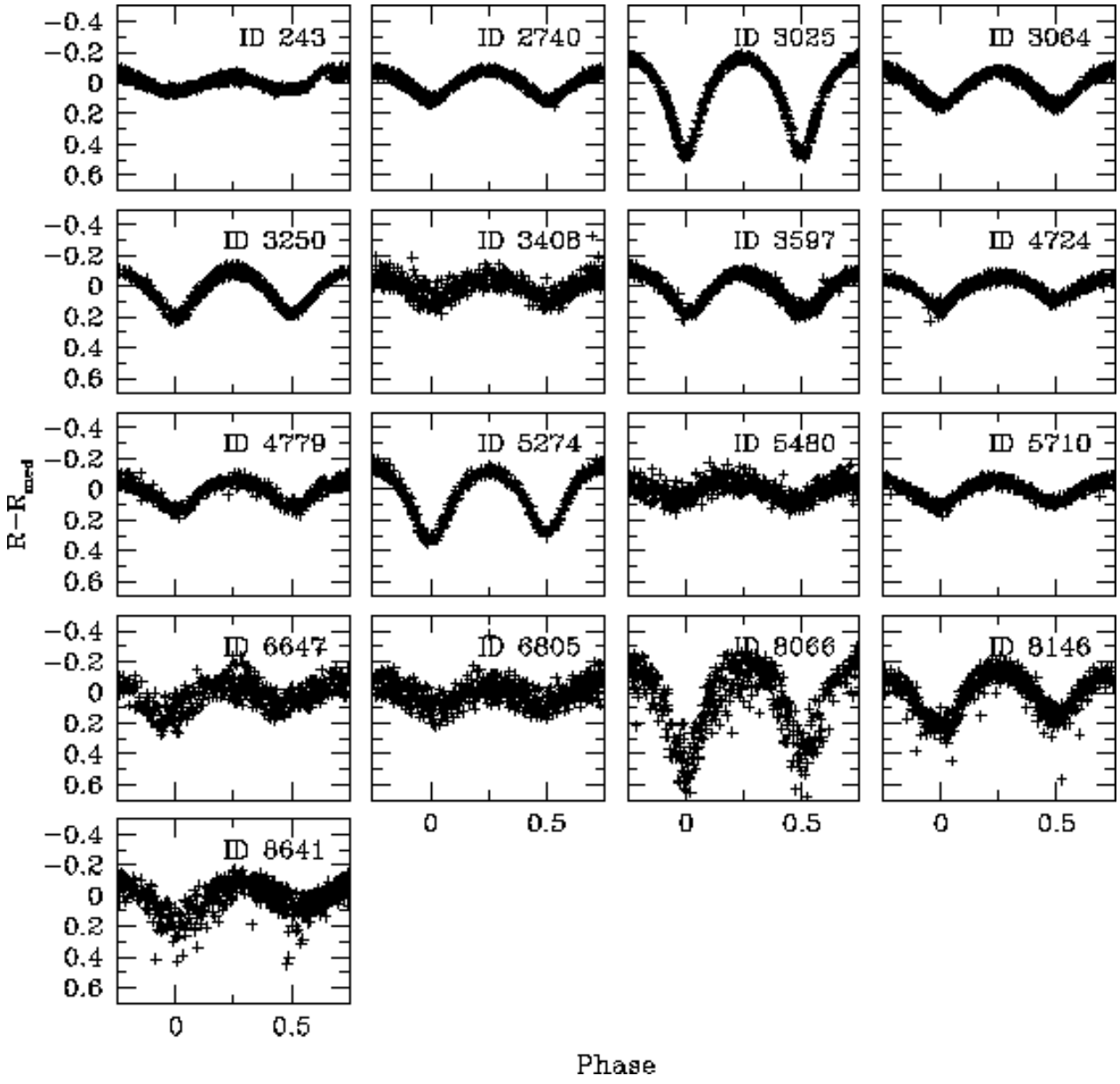

Fig. 9.— Light curves (type EW) for the W UMa variable stars detected in this study.

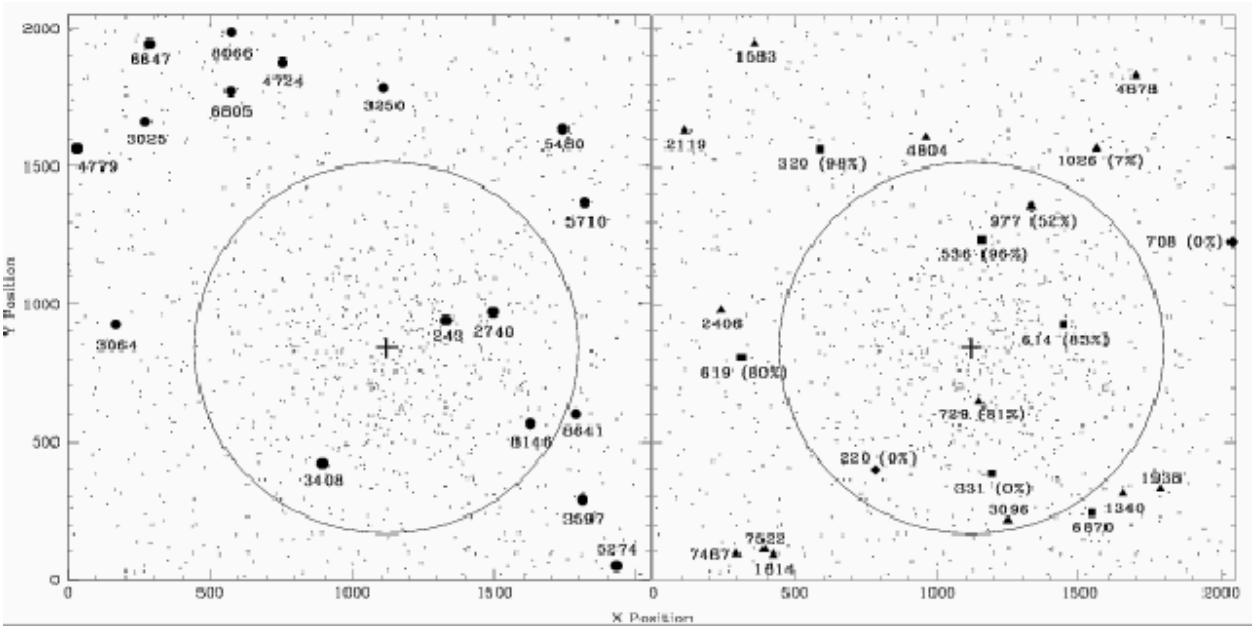

Fig. 10.— Reference frame positions for the variables detected in this study. The left panel shows the W UMa variables (*Filled Circles*) while the right panel shows the detected detached eclipsing binary systems (*Filled Triangles*), δ Scuti or pulsating variables (*Filled Square*), and unknown/unidentified variables (*Filled Diamond*). Shown for reference are stars brighter than $R = 15$ (*Small Points*) and the cluster half-mass radius ($r = 4\farcm5$; Mathieu 1984).

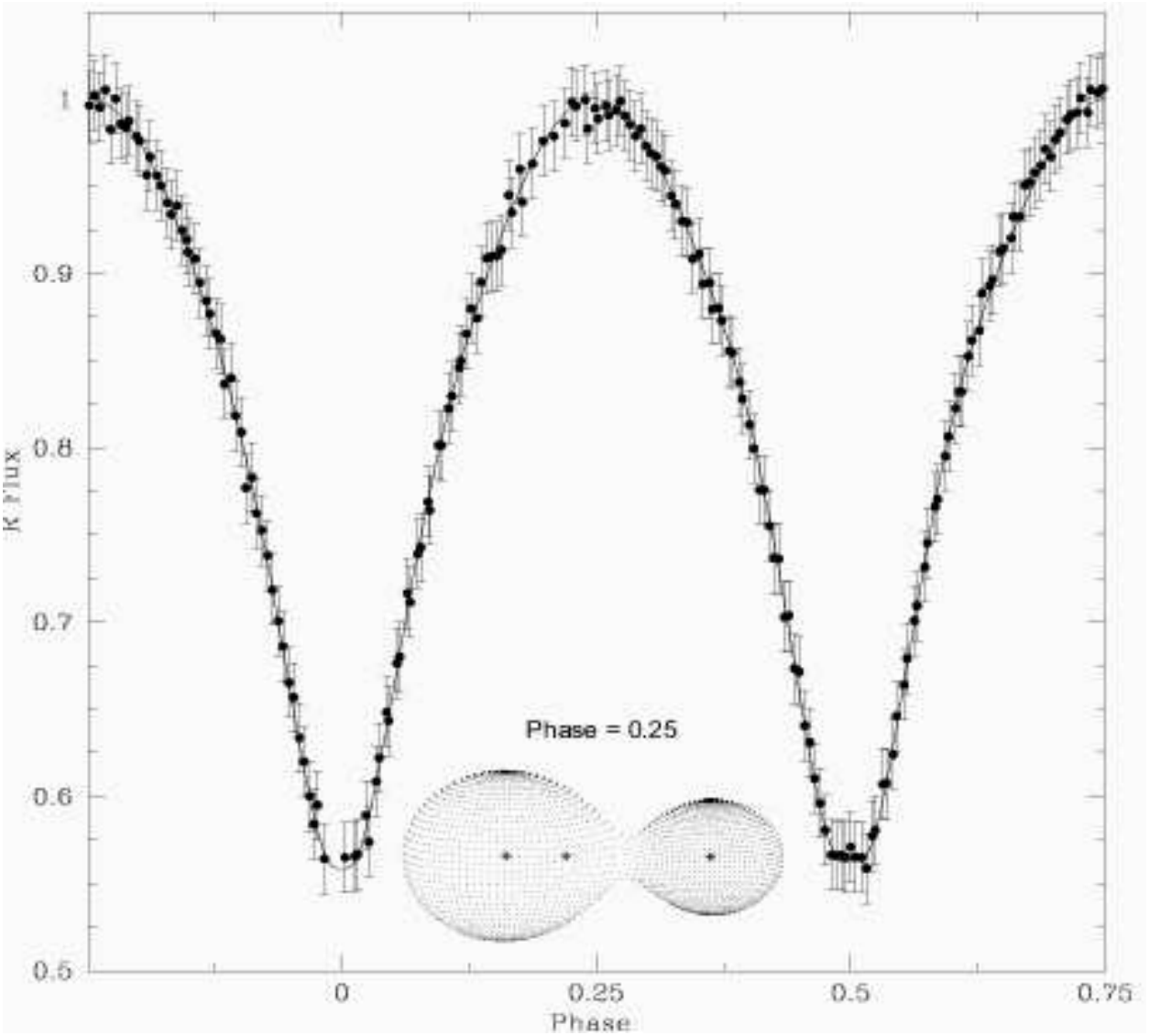

Fig. 11.— Phased light curve of ID 3025 (200 R-band normal points) shown with the adopted Wilson-Devinney differential corrections synthetic fit.

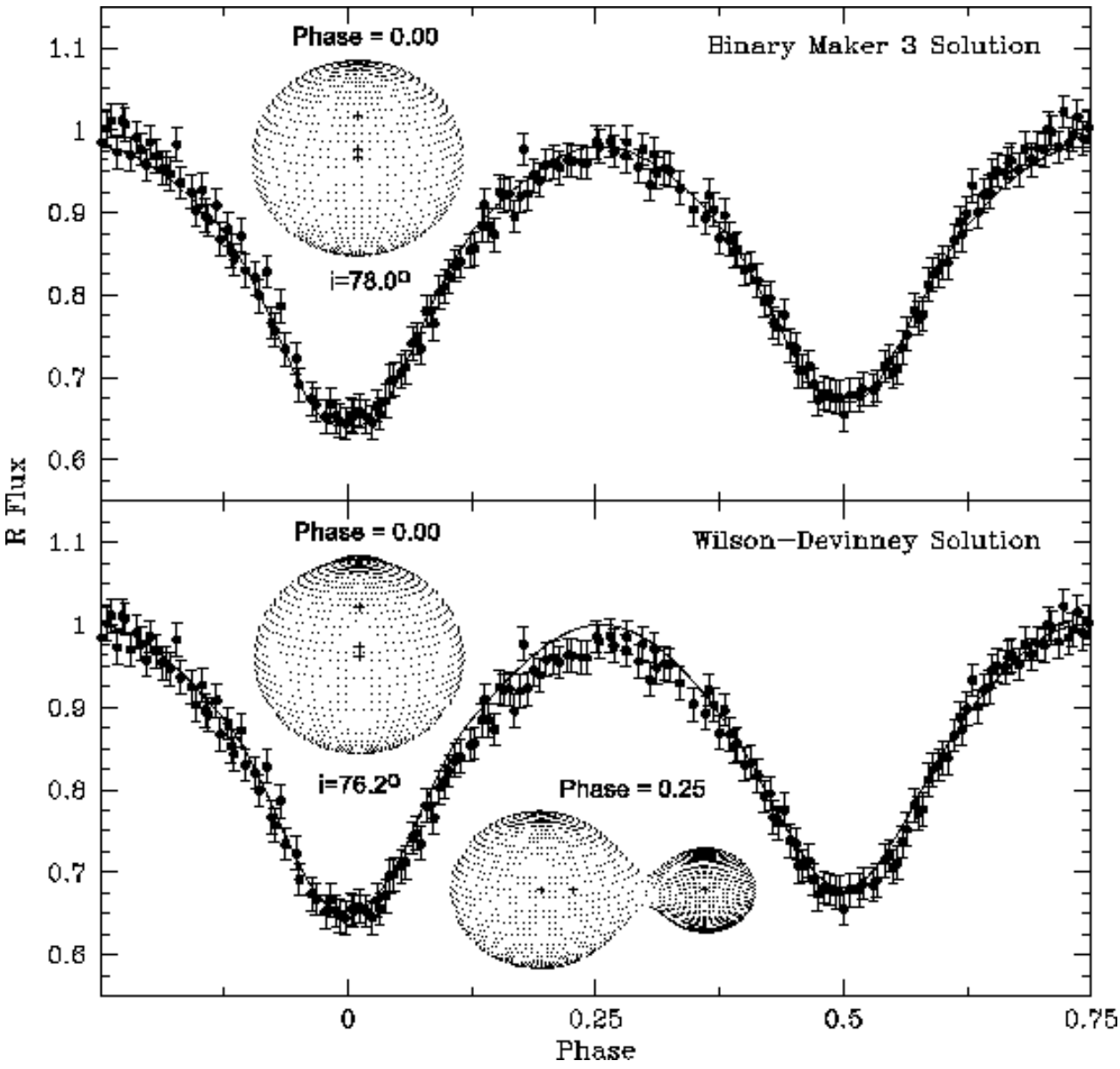

Fig. 12.— Phased light curve of ID 5274 (200 R-band normal points) shown with the (*top panel*) initial *Binary Maker 3* synthetic fit and (*bottom panel*) adopted Wilson-Devinney differential corrections synthetic fit. The 3-D models are displayed at phase 0.00 in both cases, showing that the Wilson-Devinney model just barely produces a non-total primary eclipse.

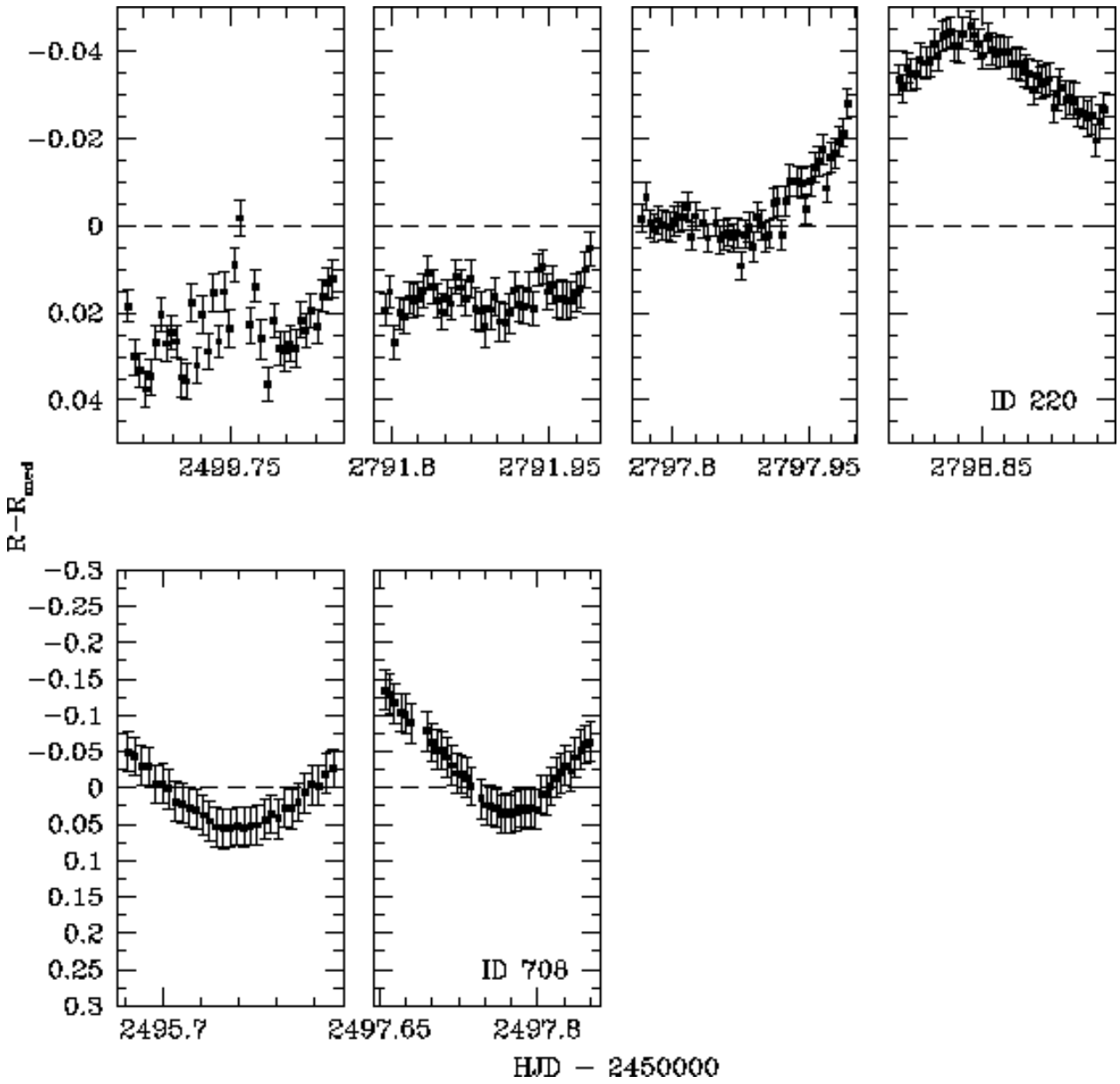

Fig. 13.— Light curves for the unknown/unidentified variables detected in this study. Four nights of data are shown for ID 220 (showing both the long and short term variations). Two nights of data are shown for ID 708.

Table 1. Observation Log for M11

UT Double Date	# Images	Average Seeing (″)
08-09 August 2002	31	2.9 ± 0.5
10-11 August 2002	40	3.8 ± 0.6
12-13 August 2002	39	4.7 ± 1.8
13-14 August 2002	38	5.0 ± 1.9
14-15 August 2002	37	4.5 ± 0.9
15-16 August 2002	35	4.8 ± 0.6
30-31 May 2003	18	4.8 ± 0.7
31-01 May 2003	45	4.9 ± 0.8
01-02 June 2003	39	6.2 ± 3.0
02-03 June 2003	48	6.9 ± 3.3
05-06 June 2003	44	6.4 ± 3.3
06-07 June 2003	50	4.9 ± 1.8
07-08 June 2003	49	4.5 ± 0.6

Note. — The photometry in this study is uncalibrated.

Table 2. Detected Variable Stars

ID	GSC,ID$_{\rm MPS}$(P%)	RA	DEC	m_V	σ_V	$m_{R_{med}}$	$\sigma_{R_{med}}$	$(V-R)_O$	I_{WS}	σ_R	T[a]
220	683(0)	18h 51m 14.8s	$-06°18'26.''3$	13.665	0.006	13.2648	0.0015	0.160	45.06	0.016	4
243	5126:4687,1268(62)	18h 51m 00.2s	$-06°14'49.''2$	13.706	0.006	13.3183	0.0050	0.110	78.94	0.041	3
320	5126:5601,1711(98)	18h 50m 43.6s	$-06°19'47.''5$	14.044	0.006	13.6210	0.0014	0.183	5.59	0.013	1
331	5126:4823,676(0)	18h 51m 15.1s	$-06°15'43.''8$	14.006	0.006	13.6330	0.0021	0.134	24.14	0.017	1
536	5126:5659,1531(96)	18h 50m 52.4s	$-06°15'59.''1$	14.339	0.007	14.0610	0.0021	0.038	10.15	0.016	1
614	5126:5664,1237(83)	18h 51m 00.6s	$-06°14'04.''4$	14.479	0.007	14.2232	0.0015	0.016	38.97	0.017	1
619	1097(80)	18h 51m 03.9s	$-06°21'35.''2$	14.595	0.007	14.2124	0.0017	0.143	57.77	0.018	1
708	1521(0)	18h 50m 52.5s	$-06°10'07.''7$	...	...	14.4427	0.0213	...	7.39	0.047	4
729	900(81)	18h 51m 08.1s	$-06°16'01.''7$	14.659	0.007	14.4220	0.0022	-0.003	46.98	0.040	2
977	1596(52)	18h 50m 49.1s	$-06°14'49.''7$	15.146	0.007	14.7862	0.0019	0.120	45.78	0.026	2
1026	1715(7)	18h 50m 43.4s	$-06°13'18.''0$	15.220	0.007	14.8742	0.0016	0.106	38.043	0.018	2
1340	...	18h 51m 17.0s	$-06°12'38.''6$	15.825	0.009	15.2757	0.0017	0.309	224.04	0.104	2
1583	...	18h 50m 33.4s	$-06°21'19.''2$	16.149	0.009	15.4925	0.0032	0.416	597.41	0.093	2
1814	...	18h 51m 23.1s	$-06°20'49.''2$	16.157	0.012	15.5967	0.0114	0.320	219.03	0.208	2
1938	...	18h 51m 16.5s	$-06°11'47.''3$	16.377	0.009	15.7942	0.0022	0.343	604.43	0.094	2
2119	...	18h 50m 41.9s	$-06°22'56.''9$	16.543	0.009	15.9045	0.0016	0.399	7.15	0.025	2
2406	...	18h 50m 59.4s	$-06°22'05.''3$	16.750	0.010	16.0339	0.0077	0.476	...	0.109	2
2740	...	18h 50m 59.4s	$-06°13'43.''5$	16.907	0.010	16.2690	0.0099	0.418	47.01	0.066	3
3025	...	18h 50m 41.1s	$-06°21'53.''1$	16.996	0.012	16.5437	0.0227	0.277	117.17	0.219	3
3064	...	18h 51m 00.8s	$-06°22'33.''6$	17.080	0.010	16.3454	0.0098	0.495	21.24	0.079	3
3096	...	18h 51m 19.7s	$-06°15'20.''8$	17.467	0.010	16.5342	0.0022	0.693	739.04	0.145	2
3250	...	18h 50m 37.7s	$-06°16'19.''2$	17.056	0.010	16.5221	0.0128	0.394	59.21	0.100	3
3408	...	18h 51m 14.2s	$-06°17'42.''2$	...	...	16.5916	0.0079	...	89.16	0.094	3
3597	...	18h 51m 17.6s	$-06°11'36.''9$	17.303	0.011	16.8114	0.0113	0.272	34.01	0.092	3
4678	...	18h 50m 36.4s	$-06°12'24.''3$	17.858	0.013	17.1555	0.0057	0.462	9.01	0.115	2
4724	...	18h 50m 35.2s	$-06°18'41.''0$	18.126	0.013	17.3207	0.0073	0.500	25.38	0.064	3
4779	...	18h 50m 43.7s	$-06°23'29.''2$	18.455	0.013	17.2955	0.0102	0.919	7.38	0.073	3
4804	...	18h 50m 42.4s	$-06°17'18.''2$	17.958	0.013	17.2570	0.0027	0.461	19.42	0.068	2
5274	...	18h 51m 24.0s	$-06°10'48.''0$	17.972	0.012	17.3137	0.0280	0.368	42.41	0.163	3
5480	...	18h 50m 41.5s	$-06°12'07.''8$	18.290	0.016	17.4844	0.0075	0.466	25.80	0.070	3
5710	...	18h 50m 48.7s	$-06°11'34.''9$	18.249	0.014	17.6210	0.0085	0.352	7.784	0.061	3
6647	...	18h 50m 33.5s	$-06°21'48.''3$	18.395	0.018	17.6968	0.0100	0.218	40.682	0.128	3
6805	...	18h 50m 38.1s	$-06°19'53.''8$	18.799	0.021	17.8643	0.0063	0.745	12.516	0.088	3
6870	...	18h 51m 18.8s	$-06°13'22.''4$	18.766	0.016	18.1076	0.0117	0.419	28.16	0.113	1
7467	...	18h 51m 23.0s	$-06°21'41.''2$	19.145	0.021	18.2640	0.0114	0.640	34.06	0.107	2

Table 2—Continued

ID	GSC,ID$_{\rm MPS}$(P%)	RA	DEC	m_V	σ_V	$m_{R_{med}}$	$\sigma_{R_{med}}$	$(V-R)_O$	I_{WS}	σ_R	T[a]
7522	...	18h 51m 22.6s	$-06^\circ 21' 01.''9$	19.115	0.021	18.1868	0.0043	0.688	45.02	0.141	2
8066	...	18h 50m 32.3s	$-06^\circ 19' 53.''4$	19.211	0.024	18.4849	0.0269	0.636	47.64	0.263	3
8146	...	18h 51m 10.2s	$-06^\circ 12' 50.''1$	19.332	0.022	18.4508	0.0170	0.760	21.12	0.132	3
8641	...	18h 51m 09.3s	$-06^\circ 11' 47.''1$	19.588	0.028	18.6337	0.0137	0.620	20.23	0.133	3

Note. — The data included in the table columns are as follows: (1) variable identification number from this study, (2) variable identification number from the *Hubble Space Telescope* Guide Star Catalog, variable identification number from McNamara, Pratt, & Sanders 1977 (membership probability given in parentheses),(3) Right Ascension (J2000.0), (4) Declination (J2000.0), (5)mean V apparent magnitude, (6) 1σ error on the mean V apparent magnitude, (7) median R apparent magnitude, (8) 1σ error on the median R apparent magnitude, (9) $(V-R)$ color index (shifted to match theoretical isochrones; see §5 for details), (10) computed value for the Welch-Stetson variability statistic I_{WS}, (11) computed value for the Stetson-J variability statistic, (12)type of variability (see footnote to column 12).

[a]Type of variable star: 1=δ Scuti or pulsating variable,2=detached eclipsing binary,3=W UMa variable,4=unknown/unidentified variable.

Table 3. Periods, Amplitudes, and Radial Distance from Cluster Center for Detected Variable Stars

ID	GSC,ID$_{\rm MPS}$(P%)	Period (d)[a]	Amplitude (mag)	r	T[b]
220	683(0)	...	0.05	3.71	4
243	5126:4687,1268(62)	0.86577(1)	0.17	1.55	3
320	5126:5601,1711(98)	0.05453(1)	0.02	5.99	1
331	5126:4823,676(0)	0.04521(1)	0.04	3.08	1
536	5126:5659,1531(96)	0.04201(1)	0.01	2.63	1
614	5126:5664,1237(83)	0.06522(1)	0.02	2.23	1
619	1097(80)	0.04154(1)	0.02	5.39	1
708	1521(0)	...	0.15	6.63	4
729	900(81)	...	0.20	1.32	2
977	1596(52)	...	0.10	3.71	2
1026	1715(7)	...	0.10	5.66	2
1340	...	3.79130(1)	0.55	5.02	2
1583	...	1.11763(1)	0.35	8.95	2
1814	...	0.70569(1)	0.50	6.83	2
1938	...	5.62050(1)	0.50	5.59	2
2119	...	...	0.10	8.53	2
2406	...	...	0.40	5.95	2
2740	...	0.39464(1)	0.30	2.65	3
3025	...	0.441864(3)	0.65	7.87	3
3064	...	0.44110(1)	0.20	6.37	3
3096	...	1.65174(1)	0.80	4.27	2
3250	...	0.35208(1)	0.35	6.28	3
3408	...	0.25532(1)	0.20	3.18	3
3597	...	0.47349(1)	0.30	5.91	3
4678	...	0.72546(1)	0.45	7.64	2
4724	...	0.41706(1)	0.20	7.32	3
4779	...	0.38382(1)	0.30	8.72	3
4804	...	...	0.30	5.21	2
5274	...	0.3468800(1)	0.40	7.56	3
5480	...	0.43009(1)	0.20	6.73	3
5710	...	0.46243(1)	0.20	5.84	3

Table 3—Continued

ID	GSC,ID$_{\rm MPS}$(P%)	Period (d)[a]	Amplitude (mag)	r	T[b]
6647	...	0.43220(1)	0.30	9.22	3
6805	...	0.34516(1)	0.20	7.20	3
6870	...	0.08081(1)	0.40	4.89	1
7467	...	...	0.30	7.43	2
7522	...	...	0.80	6.89	2
8066	...	0.42260(1)	0.70	8.46	3
8146	...	0.29357(1)	0.40	3.84	3
8641	...	0.45950(1)	0.30	4.72	3

Note. — The data included in the table columns are as follows: (1) variable identification number from this study, (2) variable identification number from the *Hubble Space Telescope* Guide Star Catalog, variable identification number from McNamara, Pratt, & Sanders 1977 (membership probability given in parentheses), (3) period (in days) of detected variability, (4) maximum peak-to-peak amplitude (in magnitudes) of detected variability, (5) radial distance (in arcminutes) from cluster center, and (6) type of variability (see footnote to column 6).

[a]Probable errors (as determined by the precision of the period search) are given in parentheses . In some cases insufficent data (lack of multiple events) prevented a period determination.

[b]Type of variable star: 1=δ Scuti or pulsating variable,2=detached eclipsing binary,3=W UMa variable,4=unknown/unidentified variable.

Table 4. Wilson-Devinney Light Curve Solution for ID 3025

Parameter	Value
Mass Ratio	0.417(2)
Period	0.4418638 d
Inclination	$82^{\circ}.52(14)$
Fillout Factor	0.245
Third Light	0.00 (assumed)
Phase Shift	0.00 (assumed)
Wavelength	6400Å
Ω_1	2.6477(48)
r_1(pole)	0.44127(118)
r_1(side)	0.47349(163)
r_1(back)	0.50528(233)
T_1	7300 K (assumed)
L_1	0.6956(12)
g_1	1.00 (assumed)
x_1	0.405 (assumed)
A_1	1.00 (assumed)
Ω_2	2.6477(48)
r_2(pole)	0.29830(99)
r_2(side)	0.31296(125)
r_2(back)	0.35532(252)
T_2	7196(7) K
L_2	0.3044
g_2	1.00 (assumed)
x_2	0.405 (assumed)
A_2	1.00 (assumed)

Note. — Parameter descriptions: Fillout Factor=parametric characterization of the equipotential surface (percentage that the surface potential lies between the inner and outer Lagrangian surfaces); $\Omega_{1,2}$=parametric characterization of the gravitational equipotential surface; $r_{1,2}$(pole,side,back)=radii along differing axes of the system; $T_{1,2}$=effective surface temperature;$L_{1,2}$=fractional luminosity; $g_{1,2}$=gravity darkening (brightening) exponent; $x_{1,2}$=limb darkening coefficient (from van Hamme 1993); $A_{1,2}$=bolometric albedo (reflection coefficent).

Table 5. Light Curve Solutions for ID 5274

Parameter	*Binary Maker 3*	Wilson-Devinney
Mass Ratio	0.25	0.236(6)
Period	0.3468800 d	0.3468800 d
Inclination	$78^{\rm O}.0$	$76^{\rm O}.16(75)$
Fillout Factor	0.25	0.468
Third Light	0.00	0.00 (assumed)
Phase Shift	0.50	0.50 (assumed)
Wavelength	6400Å	6400Å
Ω_1	2.3135	2.2501(75)
r_1(pole)	0.47892	0.49062(293)
r_1(side)	0.52012	0.53639(441)
r_1(back)	0.54701	0.56554(608)
T_1	6650 K	6550 K (assumed)
L_1	0.7377	0.7462(64)
g_1	0.32	0.32 (assumed)
x_1	0.38	0.38 (assumed)
A_1	0.50	0.50 (assumed)
Ω_2	2.3135	2.2501(75)
r_2(pole)	0.25770	0.26200(503)
r_2(side)	0.26953	0.27534(635)
r_2(back)	0.31077	0.32720(1586)
T_2	7000 K	6995(22) K
L_2	0.2623	0.2538
g_2	0.32	0.32 (assumed)
x_2	0.38	0.38 (assumed)
A_2	0.50	0.50 (assumed)

Note. — Parameter descriptions: Fillout Factor=parametric characterization of the equipotential surface (percentage that the surface potential lies between the inner and outer Lagrangian surfaces); $\Omega_{1,2}$=parametric characterization of the gravitational equipotential surface; $r_{1,2}$(pole,side,back)=radii along differing axes of the system; $T_{1,2}$=effective surface temperature;$L_{1,2}$=fractional luminosity; $g_{1,2}$=gravity darkening (brightening) exponent; $x_{1,2}$=limb darkening coefficient (from van Hamme 1993); $A_{1,2}$=bolometric albedo (reflection coefficent).